

Examining the Faraday Effect using lock in amplification

P. Oikonomou^{a,*}, M. Filova^a

^aNew York University Abu Dhabi

Abstract

An attempt to detect the Faraday Rotation of SF-57 Glass and NYUAD tap water was conducted using multiple methods. Specifically, a brute force measurement of the angle using a constant magnetic field yields the Verdet constant of SF-57 Glass to be 23.3 ± 0.3 rad/Tm, but was ineffective in providing a result for water. To detect smaller signals, an alternating magnetic field was employed and the Faraday shift was measured using a lock in amplifier. The Verdet constants obtained from this process were 24.1 ± 0.9 rad/Tm and 1.90 ± 0.2 rad/Tm for SF-57 Glass and water respectively, which were in agreement with other literature. To increase the accuracy in the measurements, as well as repeatability, additional equipment was developed to automate the process of obtaining data. Such equipment allowed us to obtain accurate measurements of the signal as a function of polarization angle, which lead to characterising the phase response of our polarizer, and introducing a correction to Malus' law in order to take into account the phase of the incoming light.

1. Introduction

Faraday effect is the phenomenon of rotation of the plane of polarization of light as it passes through a magnetic field. It was first observed experimentally by Michael Faraday in 1845 and it is historically significant as a demonstration of a connection between light and magnetism [1]. Today Faraday effect has both commercial and scientific applications. For example, Faraday rotator materials are used in optical isolators which make use of the dependence of the direction of rotation on the direction of light with respect to the magnetic field [2]. The effect has been used to design various components such as optical switchers, modulators, circulators and isolators, all widely used in laser systems and telecommunication [3]. Understanding of Faraday rotation has also been important for radio astronomy to either account for its effects [4] or use it as a tool for example to measure magnetic fields in pulsars [5].

In this experiment we use a lock-in amplifier to precisely measure the Verdet constant which quantifies the Faraday effect. Lock-in amplifiers are commonly used to extract information about signals of particular frequency and phase from noisy data [6]. Lock-in-detectors are widely used in many fields of research varying from physics, engineering to life sciences [6]. In this experiment, usage of a lock-in-amplifier provides an opportunity to gain a good understanding of its powers and functioning.

2. Theory

In this section we present the theoretical background behind all the aspects of the experiment. This includes the micro-

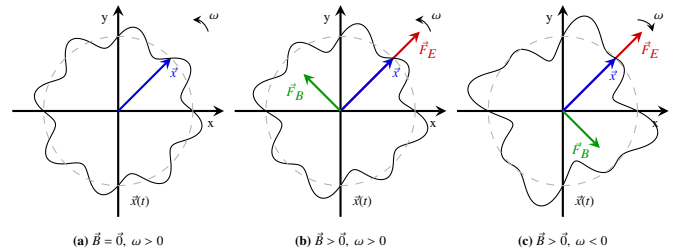


Figure 1: Intuitive picture for the oscillation of an electron due to the external electromagnetic field and constant magnetic field. The z axis is aligned parallel to the light wave propagation, and the x-y axes are for a plane perpendicular to z. (a) shows how the electron oscillates around the bound nucleus in the absence of any external field (ground oscillation). (b) shows the counter-clockwise polarized component, which induces an additional oscillation out of phase with the ground oscillation. Hence the total oscillation amplitude is reduced. (c) shows the clockwise polarized component, which induces an additional oscillation in phase with the ground oscillation. Hence the total oscillation amplitude is increased. The oscillation amplitude corresponds to the induced magnetic polarization in the medium.

physics of Faraday rotation, the operation of the lock in amplifier, as well as the theory behind the experimental AC detection of the signal.

2.1. Faraday Rotation Physics

The primary objective of this experiment is to study the effect of Faraday Rotation. Here we describe, first intuitively and then rigorously, the classical theory behind Faraday Rotation.

2.1.1. Intuitive Outline

When plane polarized light passes through a dielectric in a magnetic field, its plane of polarization appears to rotate by an angle that depends on the length of the dielectric and the magnitude of the parallel magnetic field inside. This apparent change is referred to as Faraday Rotation [7].

*Corresponding author

Email address: po524@nyu.edu (P. Oikonomou)

The key to the change in polarization angle is that linearly polarized light can be decomposed into two circularly polarized components. Hence, it is possible to think of plane polarized light, as a clockwise polarized component and a counterclockwise component, rotating perpendicular to the axis of propagation with opposite frequencies.

Now consider the motion of the electrons in the material that are bound to their atoms as the external electric field and magnetic field, pass through them. In the absence of external magnetic field, the electrons would oscillate along the axis of the circularly polarised magnetic field due to the wave. In the presence of an external magnetic field this motion is displaced, either in the same direction for the clockwise, or opposite for the counterclockwise polarized component. This induces a difference in their oscillation amplitude (See sketch in Fig. 1) [8]. As a result of the motion of the electrons, the material is polarized more in the clockwise direction and less in the anticlockwise. This leads to a difference in the amplitudes of the circularly polarized components of the light. We can now add them together after the end of the rod, to obtain a phase-shifted linearly polarized wave.

2.1.2. Mathematical Description

To rigorously show the phase shift, we will need to derive the equation of motion of the electrons due to the external electric field. Then decompose the displacement into its clockwise and counterclockwise components, calculate the polarization for both circulations, and then use them to obtain the new magnitude of the electric field for each. Throughout this calculation we assume that the electrons are bound to their nuclei in a harmonic oscillator potential at some frequency ω_0 , as well as that the z-component of their motion, the component along the direction of the light, is negligible [9].

When in the presence of an external electric field $\mathbf{E} = E_w \exp(i\omega t)$ and magnetic displacement $\mathbf{H} = H_0 \hat{\mathbf{z}}$ the equation of motion of the electron becomes the simple harmonic potential plus the Lorenz force [9].

$$m\ddot{\mathbf{x}} = -\omega_0 \mathbf{x} - e \left(\mathbf{E}_w e^{i\omega t} - \frac{i\omega}{c} H_0 \mathbf{x}_0 \times \hat{\mathbf{z}} \right) \quad (1)$$

where \mathbf{x}_0 is the initial displacement vector and c the speed of light. Now we can describe the clockwise and counter-clockwise rotation axes using the following basis shown in (2) [10].

$$\hat{\mathbf{s}}_{\pm} = \frac{\hat{\mathbf{x}} \pm i\hat{\mathbf{y}}}{\sqrt{2}} \quad (2)$$

We can now define the cyclotron frequency of the electron (3) [11].

$$\omega_c = \frac{eB}{m} = \frac{eH_0}{mc} \quad (3)$$

This makes it possible to rewrite the equation of motion in terms of the clockwise and counter-clockwise polarisation components (4).

$$x_{0\pm} = -\frac{e}{m} \frac{E_{\pm}}{\omega_0^2 - \omega^2 \mp \omega\omega_c} \quad (4)$$

Note that in (4) the \pm subscript refers to the components of that vector in the "rotating" axes $\hat{\mathbf{e}}_{\pm}$ defined in (2). This shows that the distance of electron from equilibrium is going to be different in the two circular polarizations. As a result, by expressing the dipole moment of this electron as $\mathbf{p} = ex_0$ we can define a Polarization \mathbf{P} for each component [9].

$$P_{\pm} = \frac{Ne^2}{m} \frac{E_w e^{kz-i\omega t}}{\omega_0 - \omega^2 \mp \omega\omega_c} \quad (5)$$

where N is the number density of electrons, k is the wavenumber of the incoming light wave, and z is the component along the z -axis. Using (5) we can define a new frequency called the plasma frequency (6) [11].

$$\omega_p = \sqrt{\frac{4\pi Ne^2}{m}} \quad (6)$$

Combining everything and calculating the electric field components for $z = L$ (the length of the material) we obtain (7) when we add up the circularly polarized components [9].

$$\mathbf{E}_w(z = L) = E_w \left(\cos \frac{\Delta n \omega L}{2c} \hat{\mathbf{x}} + \sin \frac{\Delta n \omega L}{2c} \hat{\mathbf{y}} \right) \exp \left[i \left(kL - \omega t + (\bar{n} - 1) \frac{\omega L}{c} \right) \right] \quad (7)$$

where Δn is the difference between the refractive indexes for each circular component, and \bar{n} is their average. These quantities are given in (8) (9) [9].

$$\Delta n \approx \frac{\omega\omega_c\omega_p^2}{(\omega^2 - \omega_0^2)^2 - \omega^2\omega_c^2} \quad (8)$$

$$\bar{n} \approx 1 + \frac{(\omega^2 - \omega_0^2)\omega_p^2}{2(\omega^2 - \omega_0^2)^2 - 2\omega^2\omega_c^2} \quad (9)$$

Finally, we have the means to quantify the angle of polarization difference $\Delta\phi$ due to Faraday rotation as shown in (10).

$$\Delta\phi = VBL \quad (10)$$

where V is the **Verdet constant** shown in (11), B is the magnetic field, and L is the length of the material that the wave is travelling through.

$$V = \frac{e\omega}{2mc} \Delta n \approx \frac{e}{2mc} \frac{\omega^2\omega_c\omega_p^2}{(\omega^2 - \omega_0^2)^2 - \omega^2\omega_c^2} \quad (11)$$

Thus, we arrive to the purpose of this experiment, which is to measure that constant using lock in amplification. Before we do that, however, it is worth discussing the phase shift of the signal. Specifically, apart from a shift in the plane of polarization of the liquid, Faraday rotation includes a phase shift of the wavelength. That phase shift $\Delta\theta$ is given by (12), and will become critical in Section 2.3.

$$\Delta\theta = \frac{2mc}{e} \frac{VL}{(\omega^2 - \omega_0^2)^2\omega_c} \quad (12)$$

2.2. Malus Law

To detect the shift in polarization angle, we are sending a polarized light wave through a material in a magnetic field and then resolve it with an additional polarizer. A more detailed description of the setup can be found in Section 3.1, however, for now, we only care about modelling the light through the polarizer.

To model that we use Malus' Law (13), which describes how the intensity varies with polarisation angle [8].

$$I' = I_{max} \cos^2 \Delta\phi \quad (13)$$

Malus law, despite its simplicity, will come up all over the report, starting from the following section. Note that Malus' Law says nothing about the phase of the light. (Spoiler-alert! this is further explored in Section 6.4).

2.3. Lock In Amplification

Verdet constants are usually of the order of 10 rad/Tm; hence, Faraday rotation is a considerably small effect to measure in a scale other than for starlight passing through the earth's atmosphere. To do the experiment we will require a more sophisticated approach towards small signal measurement. That is why we are using lock-in amplification. This section will describe the operation and structure of a lock in amplifier, as well as how it is applied on this experiment.

2.3.1. Operation of a Lock in Amplifier

The purpose of a lock in amplifier is to get the amplitude of an AC signal. Specifically, given an arbitrary signal and a reference frequency, the lock in amplifier will, essentially, decompose the signal into its frequencies and return the amplitude of the one corresponding to the reference.

To be slightly more rigorous, we can define the Fourier transform and its inverse for a function $f(t)$ in (14) and (15) respectively.

$$\mathcal{F}[f](\omega) = \int_{\mathbb{R}} f(t) e^{-i\omega t} dt \quad (14)$$

$$\mathcal{F}^{-1}[F](t) = \frac{1}{2\pi} \int_{\mathbb{R}} F(\omega) e^{i\omega t} d\omega \quad (15)$$

Now we can think of the function of the lock in, as going to frequency space through a Fourier transform, multiplying a signal with a envelope function (in this case a delta function located at the reference frequency) and returning the root mean square of the inverse Fourier transform. The envelope function of the ideal lock in would be the one in (16)

$$G(\omega) = \frac{1}{2} [\delta(\omega - \omega_r) + \delta(\omega + \omega_r)] \quad (16)$$

where ω_r is the reference frequency. Note here that we are adding two delta functions that peak at $\pm\omega_r$. That is because the Fourier transform of a pure frequency has this signature. Hence multiplying by $G(\omega)$ would only select the amplitude of the reference frequency. Thus the output of an ideal lock in

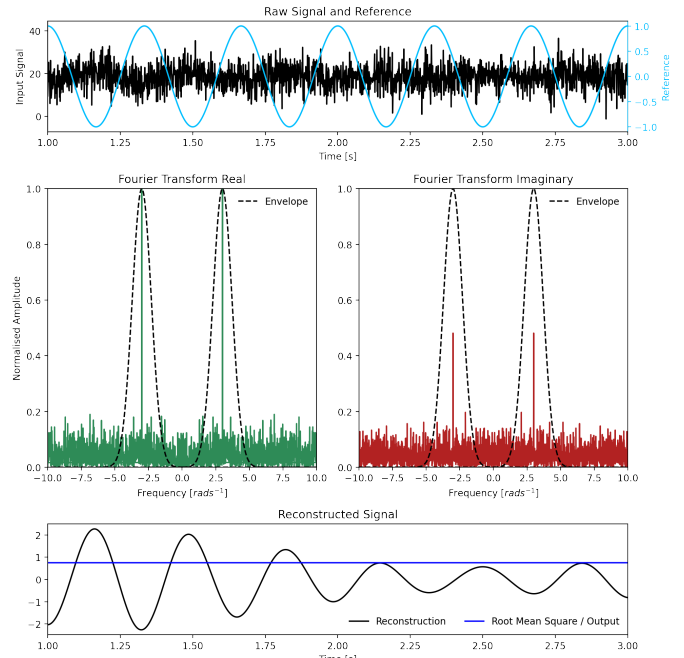


Figure 2: Example of lock in operation described in Section 2.3.1. The signal, shown in the top figure, is of the type we encountered in the experiment (For more see Section 2.3.3) i.e. a central frequency with white noise and uniform frequency noise. The reference is also shown in the top with blue. The middle two plots illustrate the real and imaginary components of the Fourier transform with respect to the phase of the reference signal. Notice that the peak frequency has a higher imaginary than real component. This results in the reconstruction (lower plot) being phase shifted with respect to the reference, thus the average signal decreased.

that receives a signal $V(t)$ and reference frequency ω_r , would be given by (17)

$$V_{loc}^2 = \frac{1}{T} \int_T \mathcal{F}^{-1} [\mathcal{F}[V(t')](\omega) G(\omega)](t) dt \quad (17)$$

Plugging in $V(t) = V_0 \cos \omega_r t + \phi$ in (17) we obtain the following result.

$$V_{loc} = \frac{V_0}{2} \cos \phi \quad (18)$$

Equation (18) reveals an important result for the lock in behaviour. Namely, that the output is proportional to the amplitude of the signal as expected, but also that it is dependent on the phase difference between the reference signal and the input signal. We will come back to this in Section 6.4, but for now, perhaps it is worth to describe a more realistic model for the lock in. To do that we introduce, instead of a delta envelope, a Gaussian envelope. Hence we can replace (16) with (19).

$$G'(\omega) = \frac{1}{\sqrt{8\pi\sigma^2}} \left[\exp\left(-\frac{(\omega - \omega_r)^2}{\sigma^2}\right) + \exp\left(-\frac{(\omega + \omega_r)^2}{\sigma^2}\right) \right] \quad (19)$$

The operation of such a lock in is shown step by step in Fig. 2

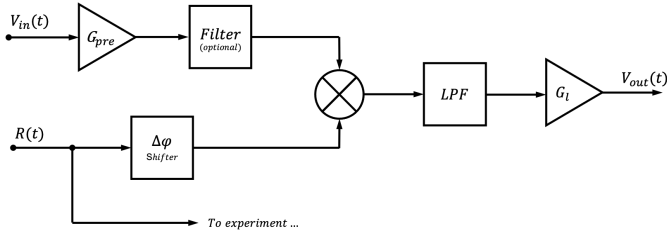


Figure 3: Lock in amplifier block diagram. The incoming signal from the experiment V_{in} is amplified with Gain G_{pre} via the preamplifier, then it is optionally filtered, and then multiplied to the appropriately phase shifted reference signal $R(t + \Delta\phi)$. Finally, a low pass filter and amplifier produce the final DC signal. This figure was created based on the description in [12]

2.3.2. Lock in Architecture

It is important to note that the discussion in Section 2.3.1 is purely mathematical and designed to offer a way to think of the operation of the lock in. In the circuit level the lock in amplifier, does not have a spectrum analyser or anything of the sort. This section analyses the actual implementation of the device.

Fig. 3 illustrates the block diagram of an implementation for a lock in amplifier. Let's start analysing it by describing the operation of the multiplier. The input signal $V_{in}(t)$ is multiplied with the phase shifted reference signal $R(t)$ (here, the R stands for reference). Note, however, that $R(t)$ is still a voltage. If these are sinusoidal signals, this seems trivial until we look at it in its Fourier decomposition. Taking the Fourier transform of their multiplication we obtain the following.

$$|\mathcal{F}[f \cdot g](\omega)| = |(\mathcal{F}[f] * \mathcal{F}[g])| \\ = \delta(\omega - |\omega_{in} - \omega_{ref}|) + \delta(\omega - (\omega_{in} + \omega_{ref}))$$

where ω_{in} is the frequency of $V_{in}(t)$ and ω_{ref} is the frequency of the reference signal $R(t)$. Note that in this calculation we are taking the magnitude of the Fourier transform, hence the effect of the phase goes away since we are summing the real and imaginary parts, however this can be brought back just as shown in Section 2.3.1.

In the case where $\omega_{ref} = \omega_{in}$ (which is the case we are interested in) we have two peaks in the transform. One at dc ($\omega = 0$) and one at their sum. The idea is that the amplitude of the dc peak is proportional to the average of $V_{in}(t)$ [13]. Hence to obtain just that peak, we pass through a low pass filter (See Fig. 3) that will cut off the peak at $\omega_{ref} + \omega_{in}$. This is illustrated in Fig. 4.

As a last note, we will show the signal prior to the low pass filter a lot throughout this report, because it conveys a lot of information about our system. This will perhaps provide greater insight why when the signal is in phase the average is proportional to the amplitude, but when the signal is out of phase the average is 0. Fig. 5 shows exactly these two cases. The odd function will have a time average of 0, while the average of the even, will be proportional to its amplitude.

2.3.3. Application to Faraday Rotation

One main important question, however, still remains. How do we apply this idea to measure the small signal of our Faraday

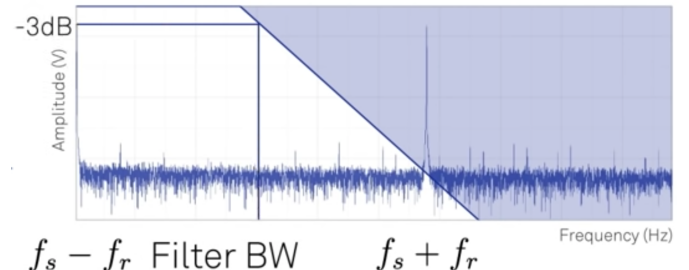


Figure 4: Illustration of signal addition in Fourier space for a lock in amplifier. The blue overlay is the blocking of frequencies for a proposed low pass filter for this application in order to provide the appropriate signal. Adapted directly from [14]

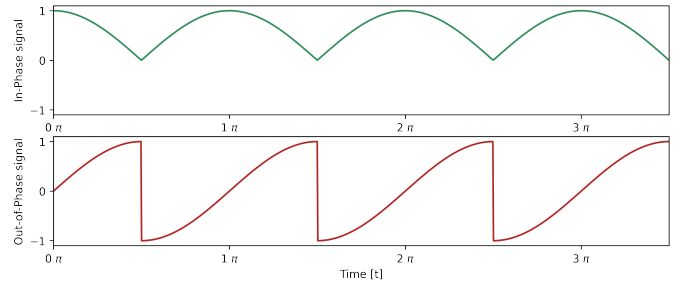


Figure 5: Illustration of the time signal in the lock in after multiplication and before the average. The top plot is the result of multiplication of two in phase signals, while the bottom plot is the result of two signals with $\pi/2$ phase difference.

rotation in the lab? This section explains how we can use an AC magnetic field and a lock in amplifier to significantly increase the accuracy of measuring Verdet constants.

As seen in Section 2.1, particularly in equation (4), at frequencies significantly lower than ω_0 and ω_c , an alternating magnetic field in the z direction, has no (first order) effect on the displacement of the electrons. Hence a slowly varying magnetic field would not change the relationship between the shift in polarisation angle and the verdet constant.

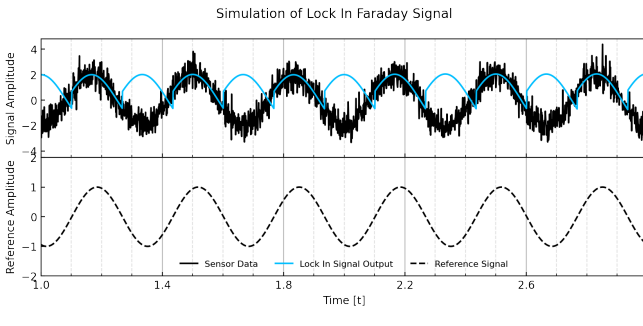
We can take advantage of this to introduce an alternating magnetic field, and measure the small change in amplitude of a photodiode signal due to the faraday phase difference using a lock in. This way, we can reject a significant amount of noise and thus detect really small oscillation amplitudes.

The math behind this methodology are as follows. Imagine that due to Faraday rotation the polarization plane changes by an angle $\phi(t)$ as a function of time, relative to some initial polarization.

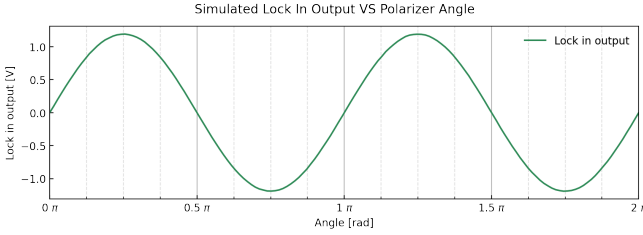
$$\phi(t) = \Delta\phi \cos(\omega t)$$

where $\Delta\phi$ is the maximum plane of polarisation angle difference due to the Faraday effect, while ω is the frequency of oscillation, which is equal to the frequency of oscillation of the magnetic field.

Now the wave passes through the polarizer which is located at an angle θ with the respect to the 0 polarization axis. Hence the signal detected by the sensor would be as seen in (20)



(a) Oscilloscope Output



(b) Signal Amplitude VS angle

Figure 6: Simulation of Faraday signal as a function of time and polarization angle. In this simulation the following parameters were used: Gain $G = 1$, Faraday Angle $\Delta\phi = 0.1 \text{ rad}$, Reference frequency $\omega = 3 \text{ rad s}^{-1}$, reference phase difference $\Delta\theta = 0.9 \text{ rad}$. (a) Shows the oscilloscope output for the polarizer set at $\theta = 45^\circ$. Gain was kept at one, to illustrate how the lock in can isolate only 1 frequency from the noise, seen by the blue curve superposed on the black. (b) Shows the lock in output, i.e. the signal amplitude as a function of polarizer angle θ . We see that the maximum occurs at $\theta = 45^\circ$ something verified experimentally in Section 5.3

$$V_{\text{sensor}}(t) = R_s k_s \frac{P}{2} \cos^2(\phi(t) + \theta) \quad (20)$$

where R_s is the resistance of the sensor (See Section 3.1 for more details), k_s is the photoreactivity of the sensor measured in A/W , θ the angle of the first polarizer, and P is the power of the laser. Then we pass the signal through the lock in shown in Fig. 3, using the current that generates the magnetic field as our reference signal $R(t)$. Hence the signal right after the low pass filter of the lock in would take the final form shown in (21).

$$V_{\text{loc}}(t) = \int_{\mathbb{R}} \mathcal{F}^{-1} [\mathcal{F}[V_{\text{sensor}}] G(\omega)] dt$$

which simplifies to:

$$V_{\text{loc}} = C_{\text{loc}} G_{\text{loc}} R_s k_s \frac{P}{2} \cos^2(\Delta\phi + \theta) \quad (21)$$

where C_{loc} is the lock in constant provided by the manufacturer and G_{loc} is the lock in gain. Finally we can estimate the Verdet constant by obtaining the amplitude of the oscillation frequency, at the polarizer angle θ at which the deflection is maximum. This would yield that, to first order, the is:

$$\Delta\phi = \frac{2V_{\text{loc}}}{G_{\text{loc}} C_{\text{loc}} R_s k_s P} \quad (22)$$

The reason why we have to approximate is because we detect V_{loc} using AC coupling. That means that the DC com-

ponent of the oscillation would be removed. This amounts to subtracting a factor of $G_{\text{loc}} C_{\text{loc}} R_s k_s P \cos^2(\theta)/2$ from (21). This would give an ugly expression to obtain the average (Notice that in (22) we have dropped the constant terms because they wouldn't be detected through AC coupling). Hence we taylor expand to first order. As a result, using (10) we can get the Verdet constant from the angle deflection $\Delta\phi$.

2.3.4. Simulation

We have developed a python module called `wfsim` that uses the theory described in Section 2 to predict the signal for this experiment. The module along with description of the code as well as examples can be found [here](#).

The simulator takes as an input the current sent to the solenoid. It then simulates the angle of Faraday deflection as a function of time, and passes it through the polarizer. Then it estimates the signal of the various electronic components using the appropriate coefficients. The simulator also takes into account electronic noise in two forms. One is white noise, essentially a gaussian sampled array of voltage deflections added to the original signal of the photodiode. The other is frequency noise. Essentially it uniformly samples frequencies in Fourier space, then takes the inverse Fourier transform and adds this noise to the signal.

We used the simulator to predict what the lock in output should be as a function of polarizer angle. In Fig. 6a we present a simulation of the lock in output for our typical setup described in Section 4.3. This allows us to see what signal we expect at a typical value for the polarizer angle θ . On the other hand, Fig. 6b obtains the lock in amplitude as a function of polarizer angle. This reveals the angular dependence of the the input amplitude, allowing us to notice that the maximum happens at $\theta = \pi/4$ as expected from Malus' law. Finally, notice the characteristic cosine of the signal as a function of the polarizer angle. This is because we assume that there is no noise whose phase depends on the angle.

3. Equipment

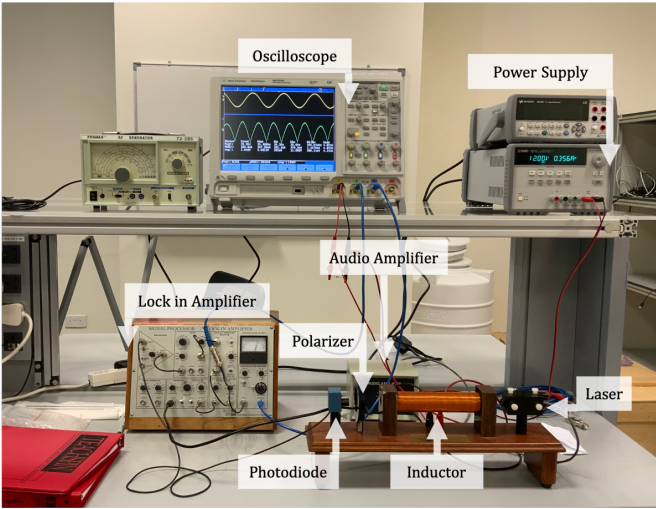
This section aims in familiarising the reader with the equipment used in our experiment, deciphering the terminology used in the rest of the report, as well as providing useful characteristics of the function of each of the components.

3.1. Teachspin Apparatus

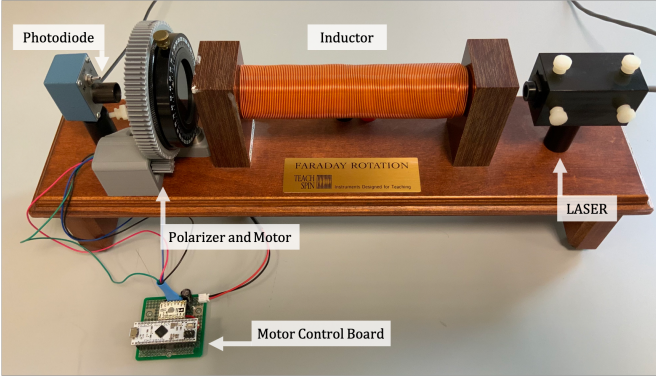
Almost all of the equipment we used for this experiment was provided by the advanced lab, and specifically the Teachspin Faraday Rotation kit. An annotated image of the complete setup is shown in Fig. 7.

The setup functions as follows. An oscillator on the Teachspin lock in amplification module generates a signal that is later amplified by the audio amplifier. A 1Ω resistor is connected in series, and the output is connected to the inductor. Parallel to the 1Ω resistor we connect an oscilloscope probe.

The laser is powered by the power supply. It has a power of $P_{\text{laser}} = 2\text{mW}$, but on its front face lies a polarizer which drops



(a) Complete Teachspin Faraday Setup



(b) Setup modifications

Figure 7: The complete setup for the Faraday experiment is shown here. Figure (a) contains the annotated setup provided to us by Teachspin. Figure (b) Contains an annotated closer view to the coil where the sample resides in, along with the modifications that we made, i.e. the polarizer motor and control board.

its intensity by half (since the initial light was unpolarized) [15]. The wavelength of the light is $\lambda = 650 \text{ nm}$ which is going to be useful in Section 6 for comparing Verdet constants among varied literature.

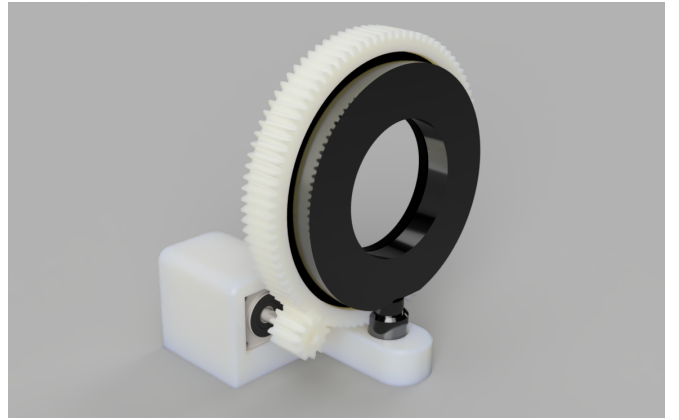
The laser light passes through an inductor made out of #18 Gauge double insulated wire, wrapped around 10 layers each with 140 turns [15]. The coil came calibrated such that the magnetic field at its center as a function of current applied is given by:

$$B = kI$$

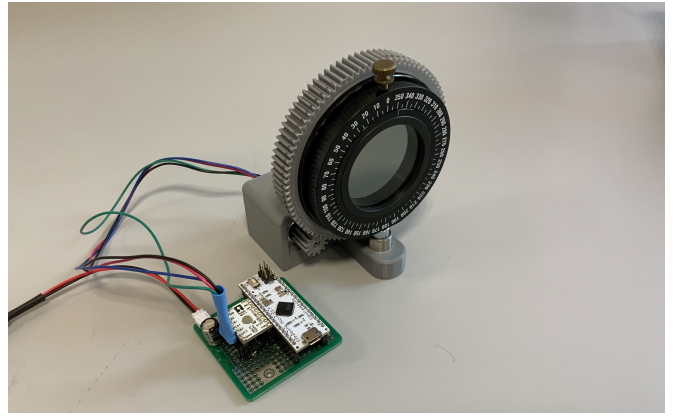
where B is the magnetic field at the center of the coil, I is the current in the coil, and $k = 11.1 \text{ mT/A}$ is a constant determined by the manufacturer [15].

The sample is located inside the inductor, and then the light passes through it and is incident on a movable polarizer with a freely adjustable plane of polarization.

After that, the light is incident on a photodiode. While it would be ideal to model the conversion of power to current using the photodiode equation, our intensity is low enough to gen-



(a) 3D Model



(b) Real

Figure 8: The 3D model of the apparatus as rendered from Fusion 360 (a), along with the real, 3D printed object (b).

erate a sufficiently small current to operate in the linear regime of the component. To ensure this, the photodiode has a resistance scale where the user can pick between $1\text{K}\Omega$, $10\text{K}\Omega$, and $100\text{K}\Omega$. Therefore, the resistor's current as a function of incident power is given by the following equation.

$$V(t) = R_p k_p P(t)$$

where $V(t)$ is the voltage across the photodiode, R_p is the selected resistance, $P(t)$ is the incident power, and $k_p = 0.6 \text{ A/W}$ is a constant known as the responsivity of the photodiode [15].

After the signal is detected by the photodiode it is sent to, either the oscilloscope (in the Case of DC measurement, Section 4.2) or to the lock in amplification module's preamplifier (in the case of AC measurement, Section 4.3).

The Teachspin Lock in amplifier module allows us to individually control the parameters of each of the stages of the lock in amplifier described in Section 2.3.2. Usually the phase sensitive detector output and the lock in output would be the signals we would monitor via the oscilloscope from this module. An example of how the lock in amplifier module is wired is shown in Fig. 10

3.2. Faraday CLI

For this experiment we wanted not only to obtain the Verdet constant but also study the phase of the incoming light after the amplification. To do this we developed some additional equipment to help us obtain measurements more effectively. Specifically, we designed a system that would operate the polarizer remotely, allowing us to perform fast, accurate, and repeatable measurements of specific polarizer angles as well as connect to the oscilloscope to obtain data in real time.

We called this system *Faraday Command Line Interface* or *Faraday CLI* and the code as well as installation instructions can be found [here](#). This section outlines the hardware design, software development, and operation mode of Faraday CLI.

3.2.1. Hardware Design

The goal of our hardware was to control repeatably and with high accuracy the angle of polarization of our second Teachspin polarizer. We essentially build a Gear that would wrap around the polarizer. A second gear was attached to a stepper motor and a cover was built to hold them all together. Everything was 3D modelled using Autodesk Fusion 360, and 3D printed in PLA using an Ultimaker 2.0 3D printer. 3D renders as well as the final result are shown in Fig. 8a. Furthermore all the 3D files can be found in our git repository [here](#).

The reason why we used a stepper motor was because of its ability to provide a constant step size. Specifically a stepper motor divides the circle into N steps, and with very high accuracy will have turned by 2π after N steps. Also, this type of motor has an active idle states. This means that when the motor is not moving, current goes through it to ensure it remains stable. The motor we picked was [this](#) 3.9V 1A 200 step motor sold by pololu. We also used a suitable driver circuit [DRV8834](#). This was a low voltage, high current, stepper motor driver, that is basically an H-Bridge breakout board, including the appropriate capacitors and resistors to be controlled by an Arduino. Since this motor would only give us 200 steps in a circle we designed the gear ratio to be 7.5 such that we turn the polariser slowly enough with each step, allowing us really fine control of the polarizer angle.

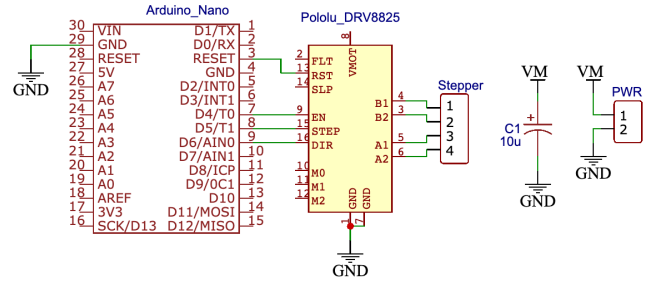
For the control board, we wanted a high clock rate processor, with small footprint, hence we used an Arduino Nano found [here](#). The overall circuit schematic as well as the circuit board we built are shown in Fig. 9a and Fig. 9b respectively.

3.2.2. Software Development

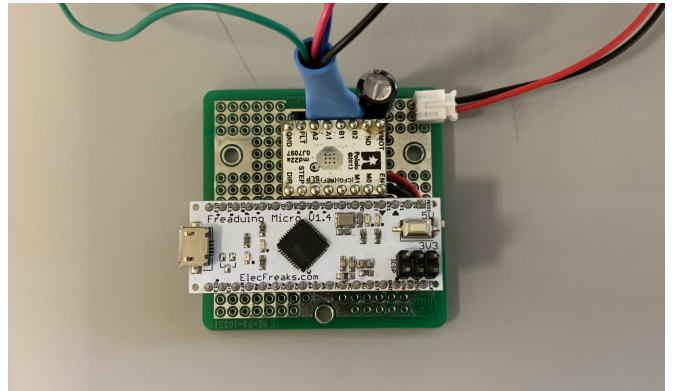
The bulk of this project was the software. The software had to perform 3 operations.

1. Control the angle of the polarizer
2. Obtain Data waveforms from the oscilloscope in real time.
3. Have a real-time command line interface to do all this, as well as a programmable interface to write scripts for certain experimental procedures.

To do that we developed 2 python libraries. One is [oscillosvisa](#), and it handles all the communications between the computer and the oscilloscope. Specifically, it handles queries to



(a) Circuit Diagram



(b) Circuit Board

Figure 9: The Circuit Diagram for the driver circuit including the Arduino and all available connectors is shown in (a). VM represents the power supply from the motor. The stepper motor coils are connected to pins 1,2,3, and 4. The real circuit board soldered together on a perfboard is shown in (b).



Figure 10: Sample setup of the Teachspin Lock in Amplification Module with a low pass filter. Blue cables go to channels of the oscilloscope (not shown). To obtain the setup without the low pass filter, we simply bypassed said component entirely.

return waveforms from selected data channels, with specific parameters.

The other library developed is [clilib](#). Clilib has a set of functions that allow one to connect to the oscilloscope, and the Arduino board and control certain attributes. A full list of commands, as well as their functionality is shown in [Appendix A](#).

perhaps here is the appropriate place to describe how commands are communicated between the oscilloscope or arduino and the computer. To do that we developed a communication protocol specifically for the type of commands listed in [Appendix A](#). The protocol is facilitated through reading and writing to and from the serial bus between the connected device and the computer. Specifically we are sending 7-byte messages of the following form.

AAXXXX\n

The encoding is as follows. The first two bytes of the message (AA) are two integers with the command code. For example to set the motor speed the code is 11. The next 4 bytes (XXXX) encode the numerical value passed to the command. The last byte is always a new line character which acts as an error detection bit. If the Arduino or the computer does not receive it, then the command will be discarded. A list of the fundamental commands and their numerical decipher chart is shown in Table 1.

AA	Description
10	Set Current angle to XXXX
11	Set the motor speed to XXXX
20	Move polarizer to angle XXXX
21	Move polarizer by angle XXXX clockwise
22	Move polarizer by angle XXXX counterclockwise
30	Send the Arduino's angle through the serial port
-1	Do not send this command to the Arduino

Table 1: Table to decipher the messages send to the Arduino. For example, in order to move the polarizer by 30 degrees clockwise the computer would send the message '210030\n'.

To communicate with the oscilloscope we used [VISA](#) as our communication protocol. It is a communication protocol that most scientific instruments support for controlling them through a serial port. We used the python library [pyVisa](#) (which was not developed by us) to send and receive visa signals.

After building the two libraries we used them to create an application [Faraday CLI](#). Faraday CLI, is a command line interface that allows the user to connect in real time with the oscilloscope and arduino through a serial protocol. It supports functionality for all the commands listed in [Appendix A](#), fully configurable and parameterisable to quickly obtain data.

If the user, however, wants to have more control, since we build the libraries in python, it is possible to program a script just as easily in order to execute a procedure repeatably. To obtain measurements for our case we wrote the script shown in full in [Appendix B](#). This script, given a range of angles, and an angle step, moves the polarizer sequentially, collects the selected

waveforms from the oscilloscope, which it saves as individual '.csv' files and then plots the output lock in signal in realtime as a function of angle. As a result, to collect 360 data point takes only 1 minute and 30 seconds, whereas in our previous method, to collect 20 data points took almost an hour!

4. Methodology

In this section we describe the methodology we used to perform the measurements: modeling the polarizer with Malus's law, finding the Verdet constant of a glass rod and water with DC current and with AC current.

4.1. Malus' Law

First, we modeled the polarizer and photodetector response with Malus's law. As explained in Section 2.2, Malus's law describes the change in light intensity of plane-polarized light after it passes through a polarizer, as a result of the angle difference between the transmission axis of the polarizer and the plane of polarization of the incoming light.

To obtain Malus's law we collect data for the light intensity, as measured with the photodetector at various polarization angles. Specifically, we followed this procedure:

1. Ensure that there are no samples inside the coil and that no current is sent to the coil.
2. Align the laser beam at the center of the photodetector.
3. Place the stepper motor and polarizer at the setup. Set the polarizer at angle zero.
4. Connect the photodetector output to the oscilloscope.
5. Collect data for the photodetector response for 360 angles using the script shown in [Appendix B](#). In addition to saving the data, this script generates the average value and standard deviation of the voltage signal obtained at each angle.

4.2. DC Verdet Constant

As a first measurement of the Verdet constant of a glass rod we used the DC current approach. The magnetic field created from the current through the coil creates a shift in the polarization plane (as described in Section 2.1). We measure the angle difference by recording the voltage signal with and without current and converting it to angles using Malus's law. From this we find the Verdet constant at different current values.

Specifically, we followed the procedure outlined below:

1. Place the glass rod inside the coil.
2. Align the laser at the center of the photodetector.
3. Connect a DC power supply to the coil and a digital multimeter in order to monitor the current being sent.
4. Connect the photodetector output to the oscilloscope.
5. Place the polarizer at angle 40°.
6. Set the power supply to some value that generates appropriate current (we started with 300 mA). Record the current average and standard deviation from the digital multimeter.

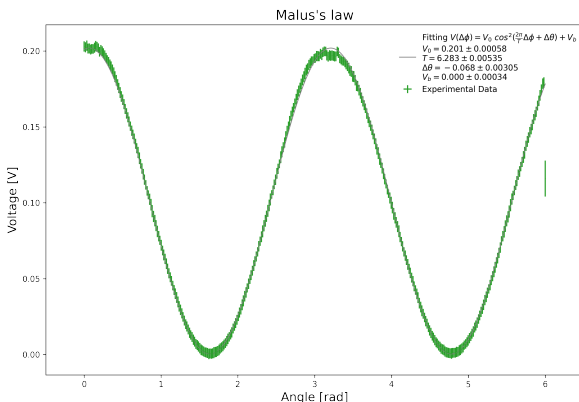


Figure 11: Fitting Malus’s law to the obtained data for calibrating the photodetector. The photodetector voltage signal was obtained at different angles of polarization by rotating the polarizer with the stepper motor.

7. Read the voltage average and standard deviation from the oscilloscope.
8. Turn off the power supply and record the average and standard deviation of the voltage signal from the oscilloscope for zero current.
9. Repeat steps 5 - 8 for several current values.

4.3. AC Verdet Constant and Phase measurements

We attempted to obtain the Verdet constant of the Schott SF-57 Rod that came with the Faraday Rotation Kit, as well as plain tap water from the lab’s endless supply of barely potable water. We did this twice, once with a low pass filter between the preamplifier and the lock in detector, and one without.

To obtain measurements we followed the procedure below. The circuit diagram is shown in Fig. 3, while the actual circuit and setup is shown in Fig. 10.

1. Set up the circuit shown in Fig. 3 on the teachspin Lock in detection module. Note that the values of the Gains are presented in the results all four experimental runs.
2. Place the sample inside the coil.
3. Align the laser source such that the beam hits the center of the detector.
4. Connect a $R = 1 \Omega$ resistor in series with the power supply and the coil. Then connect in parallel to that resistor an oscilloscope probe. That way, the voltage measured by the oscilloscope would be the current in the wire in Amperes.
5. Connect the output of the lock in detector to one channel of the oscilloscope. That way we can have the lock in values available for data processing.
6. Connect the output of the lock in amplifier module to the oscilloscope, to record the amplitude of the lock in.
7. Because the ground of the apparatus was faulty, we noticed that even before we turned on the sensor, we detected a sinusoidal signal at the frequency of the current source from the preamplifier. To remove this systematic noise, we

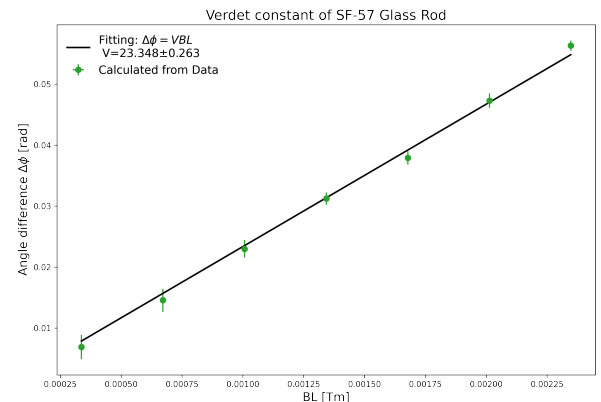


Figure 12: Finding the Verdet constant of glass rod using the DC current approach. Measurements of the voltage difference with and without current were taken at several current values. This figure shows the calculated angle difference from voltage, as a function of the magnetic field. The slope is the measured Verdet constant of glass rod.

covered the sensor with a piece of black plastic and then adjusted the offset setting on the last element of the lock in amplifier such that the output signal is 0.

8. Turn on the laser and placed the polarizer at approximately a 45 degree angle, in order to align the phase of the lock in detector. To do that look at the waveform on the oscilloscope of the lock in output and use the phase shifter to shift the phase of the reference signal such that the output looks like Fig. 5.
9. Finally, we placed the polarizer with the stepper motor and executed the script shown in Appendix B to collect data for each polarizer angle.

It is worth noting that because the data we collected for obtaining the Verdet constant was for a range of angles of the polarizer, we can use the same data to study how the phase of the light changes with the polarizer as a function of angle.

5. Results

In this section we present all the results form our experiment, as long us with some discussion on error analysis and fitting for each.

5.1. Malus’ Law

Here we present the results from calibrating the photodetector and polarizer, using Malus’s law. The methodology for this can be found in Section 4.1. The raw data and analysis can be found [here](#).

The value of the voltage signal at different angles of the polarizer is shown on Fig. 11. The data was fitted with a general function that follows Malus’s law, usng non-linear least squares fitting:

$$V(\phi) = V_0 \cos^2\left(\frac{2\pi}{T} \phi + \Delta\theta\right) + V_b \quad (23)$$

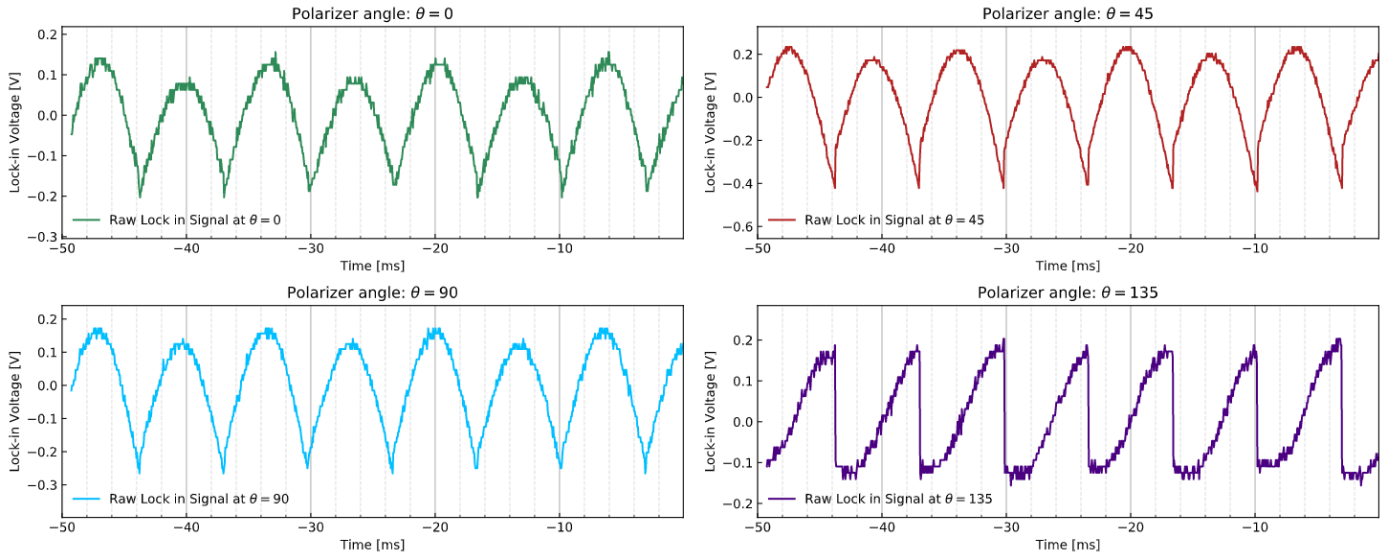


Figure 13: A series of waveforms exactly as they appeared in the oscilloscope. These waveforms show the output of the phase sensitive detector at various angles of the polarizer whilst measuring the Verdet constant of the SF-57 Glass Rod. Note how the signal is in phase at certain angles, but out of phase in others. This is the experimental version parallel to the simulation shown in Fig. 6a. A full display of waveforms can be found [here](#).

where ϕ is the angle at which the polarizer is set via the stepper motor, $\Delta\theta$ is the angle difference between the transmission planes of the polarizer in front of the photodetector and the polarizer inside the laser source, and V_b is a possible background signal that's not dependent on the laser output.

The important quantity from measuring the Malus's law is the angle difference $\Delta\theta = -0.068 \pm 0.003 \text{ rad}$. This is used later on to find the change in angle ϕ from the voltage signal.

The plotted experimental error bars are the standard deviation of the photodetector voltage signal as recorded at each angle. The errors on the parameters were computed from the estimated covariance matrix that is automatically generated by the fitting function SciPy.Optimize.Curve_fit, as the square root of the relevant element in the main diagonal:

$$\Sigma(\phi, V) = \begin{bmatrix} \sigma_{V_0}^2 & & & \\ & \sigma_T^2 & & \\ & & \sigma_{\Delta\theta}^2 & \\ & & & \sigma_{V_b}^2 \end{bmatrix} \quad (24)$$

5.2. DC Verdet Constant

Here we present the results from measuring the Verdet constant of the rod with sending DC current through the coil. The methodology for this can be found in Section 4.2. The raw data and analysis can be found [here](#).

The recorded voltages with and without current are related to the angle of the plane of polarization of the light with Malus' law (23). From the ratio V_i/V_f we can extract the change in angle of polarization ϕ as the following:

$$\phi = -\phi_0 + \Delta\theta + \arccos \cos \phi_0 + \Delta\theta \sqrt{\frac{V_f}{V_i}} \quad (25)$$

where $\phi_0 = 0.6981 \pm 0.0009 \text{ rad}$ is the angle at which the polarizer is set initially, $\Delta\theta = -0.068 \pm 0.003 \text{ rad}$ is the angle

difference between the two polarizers obtained in Section 5.1, V_f is the recorded voltage with DC current and V_i is the voltage without current.

To find the Verdet constant we plotted the calculated angle difference as a function of the magnetic field and found the slope. As shown on Figure 12, the Verdet constant was found as $V = 23.3 \pm 0.3 \text{ rad/Tm}$. The plotted error bars were propagated from the obtained data, while the error on the Verdet constant is the square root of the estimated covariance matrix.

5.3. AC Verdet Constant and Phase Measurements

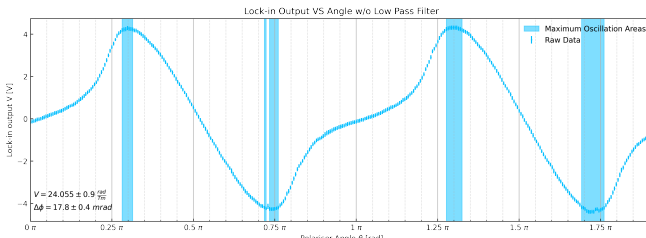
Here we present the results obtained from attempting to calculate the Verdet constant of water and the rod through the procedure outlined in Section 4.3. A set of sample waveforms of the lock in phase detector at various polarizer angles is shown in Fig. 13. These were taken whilst measuring the Verdet constant of the glass rod. A full display of waveforms can be found [here](#).

For the measurements of the rod and water we obtained the plots shown in Fig. 14 and Fig. 17 respectively. To calculate the maximum lock in voltage, we took the average of all points on the waveform whose absolute value was above 99% of the maximum. These points are shown in the shaded regions.

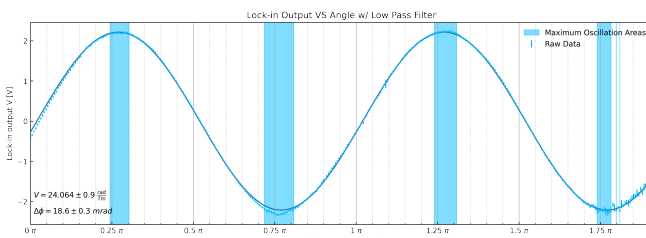
Tables C.4 and C.5 show the values of all the constants related to the setup of the equipment. Specifically they contain the gain values for each stage of the Teachspin lock in module, as well as settings, such as the resistance of the photodiode, RMS current in the solenoid, etc.

The code needed to generate these plots can be found [here](#). The entirety of the AC analysis is performed in python.

To propagate errors we used equations (10) and (22) and calculated their normal standard error with equation (26). Therefore for some quantity f that depends on some normally distributed variables x^i .



(a) Without Low Pass Filter



(b) With Low Pass filter

Figure 14: Lock in output voltage (proportional to the amplitude of oscillation due to faraday rotation) as a function of polarizer angle θ for the glass SF-57 rod. The shaded regions are the ones where the points were used to calculate the maximum values of the oscillation. Part (a) shows the results of the no-low pass filter, while part (b) shows the results with the low pass filter. The code needed to generate these plots can be found [here](#)

$$\sigma f^2 = \left(\frac{\partial f}{\partial x^i} x^i \right)^2 \quad (26)$$

As a result, Table 2 shows the Verdet constants calculated with this methodology.

Sample	Value	Unit
SF-57 Glass Rod (no LPF)	24.1 ± 0.9	rad/Tm
SF-57 Glass Rod (LPF)	24.1 ± 0.9	rad/Tm
Water (no LPF)	1.93 ± 0.1	rad/Tm
Water (LPF)	1.90 ± 0.2	rad/Tm

Table 2: Experimental measurements of Verdet constants for two samples using two different methods. LPF stands for low pass filter

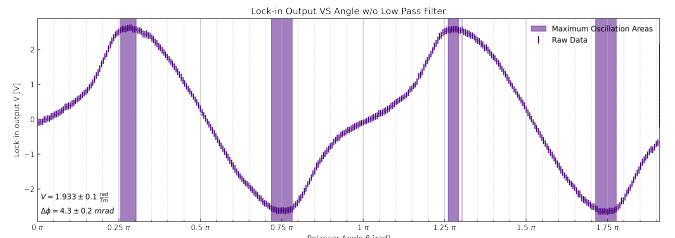
6. Discussion

Perhaps the longest section of the report. Here we discuss all the findings.

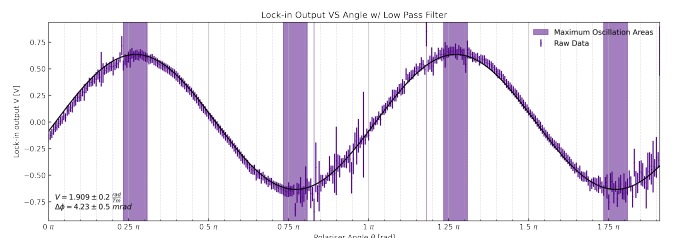
6.1. Malus' Law

As expected, χ^2 analysis confirmed that the Malus' law fit presented in Figure 11 the collected data well ($\chi^2=0.689$). This allows us to use the generated parameters in later sections as a model for the polarizer-photodetector.

Initially, we realized that the stepper motor was in fact not completing a full circle of 360 degrees after the 360 steps taken. To find the angle at which it stopped we plotted the uncertainty on the fit parameters to the Malus's law when the frequency



(a) Without Low Pass Filter



(b) With Low Pass filter

Figure 15: Lock in output voltage (proportional to the amplitude of oscillation due to faraday rotation) as a function of polarizer angle θ for water. The shaded regions are the ones where the points were used to calculate the maximum values of the oscillation. Part (a) shows the results of the no-low pass filter, while part (b) shows the results with the low pass filter. The code needed to generate these plots can be found [here](#)

$w = 1$. For all parameters minimum uncertainty occurred at angle 343 deg so we concluded that the stepper motor cycle was between 0 deg and 343 deg. The data presented in Section 5.1 is with angle values adjusted in this range.

6.2. DC Verdet

The measured Verdet constant of Glass rod of SF-57 Glass Rod is in agreement with the literature values (see Table 3).

6.3. AC Verdet

As seen in Table 2 we list the Verdet constants that we have experimentally obtained using the equipment we built (Section 3) and the methodology presented in Section 4.3. Table 3 shows the Verdet constants of the two materials as described in literature.

Sample	Value	Unit
SF-57 Glass Rod [16, 17]	23.0	rad/Tm
Pure Water [18]	3.35	rad/Tm
Pure Water [19]	2.97	rad/Tm

Table 3: Verdet Constants as described in literature, at $\lambda = 650 \text{ nm}$

Our value is in agreement with the literature values for the Schott SF-57 Glass rod. However, we do end up seeing a discrepancy for the Verdet constant of water. This is to be expected, as our water sample was nothing but distilled. We literally just filled the tube up with tap water. The tap water on campus is known to require constant filtration because of its high level of saline impurities. Such impurities would impact

the Verdet constant. Specifically, we expect to have a decrease in the value of the Verdet constant since the mass of the charged molecules in the material is greater (because of the impurities). Hence from (11) we see that the Verdet constant has an overall dependence on the mass $1/m^2$. Therefore, we can justify heuristically that our Verdet constant must indeed be smaller than the literature values.

Finally, any deviations from the literature values, could be due to the fact that we did not have the resources to calibrate our equipment in the lab. Specifically, we assumed the value of the magnetic field per current at the center of the coil, the power of the laser, etc. according to the manufacturer's manual. However, we expect that production flaws would change these values.

6.4. Phase Shift

Obtaining values for the Verdet constant of different materials is interesting, however, our apparatus allowed us to gain further insight on the subtle effect that usually goes unmeasured; the phase shift of the light as a function of polarizer angle. This section describes what phase change the setup is capable of measuring, and attempts to explain its origin.

The first question to address is what type of phase shift can the lock in detect. In Section 2.3 we describe the phase sensitivity of the lock in amplifier. Specifically, the more the signal is out of phase with the reference the more the amplitude of the lock in amplifier goes to zero. In our simulation, shown in Fig. 6b, we showed that simply following Malus' law, the phase of the signal to the lock in will not change up until a 180° phase shift occurs when the polarizer axis is parallel to the light polarization axis. That leads to the characteristic cosine that we predicted in Fig. 6b with our simulation, and experimentally confirmed with Fig. 14b and Fig. 15b.

However, notice that we were only able to obtain the pure sine plots after passing the signal through a low pass filter. Before the low pass filter was applied we would obtain a, still periodic, but slightly altered sinusoidal wave. Fig. 14a and Fig. 15a show this shape.

6.4.1. Shape of Background Signal

This oscillation pattern looks like someone added a sinusoidal signal of double the frequency on top of our normal lock in output VS polarizer angle plot. In fact, taking the Fourier transform of the data shown in Fig. 14a confirms that. The Fourier transform is shown in Fig. 16.

Fig. 16 is very insightful in figuring out what signals other than the expected dominant frequency constitute our obtained waveform. Specifically, we see, as expected, that the dominant frequency is at π while there are other frequencies at multiples of π . This is very exciting since we now have a tool to reproduce the phase response of the mysterious background signal! Taking the inverse Fourier transform of the data shown in Fig. 16 without the dominant peak we obtain the waveform for the background signal. This is shown in Fig. 17a. To ensure that this is the true background, we subtract it from the data shown in Fig. 14a to obtain Fig. 17b.

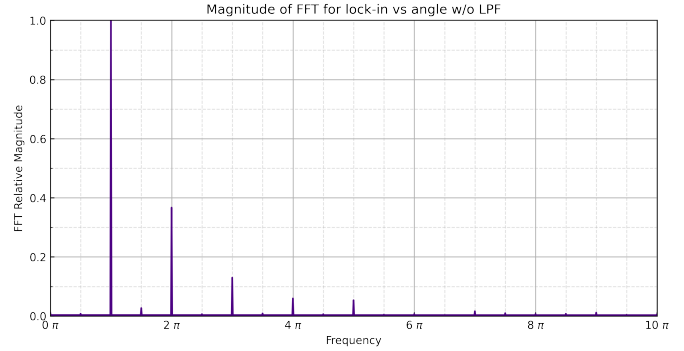


Figure 16: Fast Fourier transform of the signal vs polarization angle plot shown in Fig. 14a. Here we plot the amplitude of the Fourier transform to show the signal frequencies that are present.

6.4.2. Origin of Background signal

So far we have found the shape of the signal that changes the expected lock in signal (See simulation in Fig. 6b). We have not, however, described the origin of the signal, or what it represents.

To describe where the signal comes from we need to think about what would decrease the amplitude of the lock in. As shown in Section 2.3.1 the amplitude of the lock in amplifier would decrease either by an overall decrease in voltage, or by a phase shifted waveform at the reference frequency. In our case, since we have a signal that does not change amplitude as dramatically, we are looking at a signal whose phase is changing as a function of the polarizer angle. Specifically, such a signal, in the time domain, would be of the form shown in (27) to first order.

$$B(t, \theta) = \cos(\omega t + \alpha \sin(\beta\theta)) \quad (27)$$

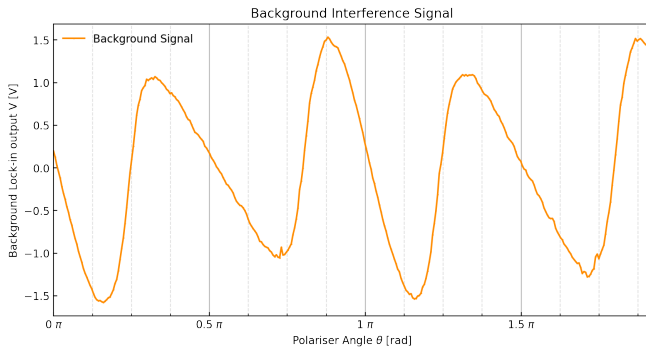
where θ is the polarizer angle, and α is some constant denoting the amplitude of the phase shift.

We now recall from Section 2.2 that Malus' law does not specify how the polarizer would alter the phase of the signal. It only specifies what the amplitude of the intensity is going to be after passing through the polarizer. What we are looking at Fig. 17a is the actual phase response of the polarizer. In other words it shows us how is the phase of the incoming light affected as a function of polarizer angle.

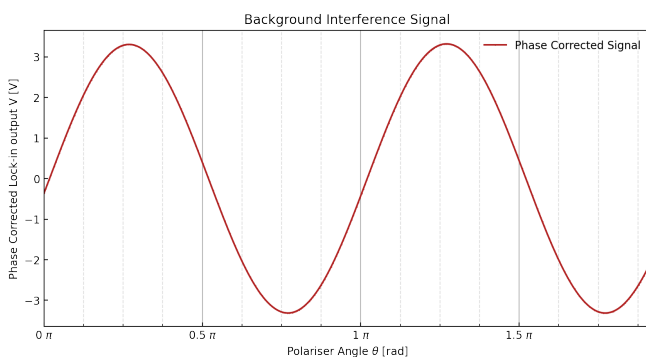
As a result, calling that waveform $F(\theta)$, we can introduce a correction Malus' law for this polarizer to obtain the phase. The updated Malus is shown in (28)

$$P(t, \theta) = P_0 \cos(\omega t + F(\theta)) \cos^2 \theta \quad (28)$$

Finally, to ensure that we are not creating physics out of thin air, we used (27) to simulate the effect of such a background signal on our measurements, without the low pass filter. The output of the simulation is shown in Fig. 18. And as expected we get a signal similar in shape to Fig. 14a and Fig. 15a.



(a) Background lock in signal



(b) Phase corrected lock in signal

Figure 17: Part (a) shows the background signal obtained by inverse Fourier transforming Fig. 16 without the dominant peak. To verify that this is the background signal we subtract it from Fig. 14a to obtain (b), which as expected is a cosine. The code needed to generate these plots can be found [here](#).

7. Conclusion

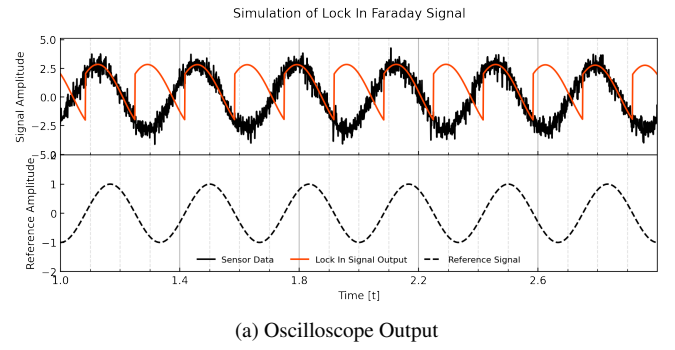
In this experiment we calculated the Verdet constant of an SF-57 Glass rod and water using direct observation through DC methods as well as AC lock in amplification. Our constants were in agreement with past experimental values obtained by both the previous groups that performed this experiment as well as existing literature.

To perform said measurements we developed some additional hardware and software to obtain more accurate raw data. Specifically, we created a control system for a polarizer as well as the necessary software to control the motor and relevant scientific instruments such as Oscilloscope and power supply. The software can be found here: https://github.com/PanosEconomou/advanced-lab/tree/main/2.Faraday-Rotation/2.Code/Faraday_Controller.

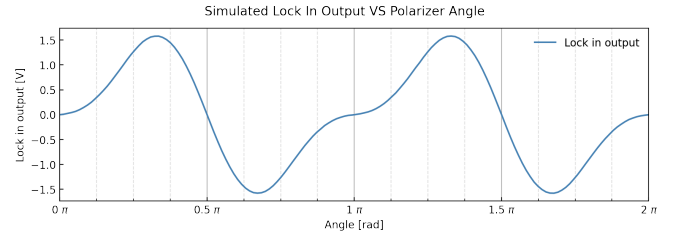
Because of the increased accuracy that the measuring equipment allowed for we were able to quantify the phase shift of the light wave passing through the polarizer, and introduce a correction to Malus' Law to take into account said phase shift.

Given more time, we would suggest the following areas for improvement.

1. Use the improved technique to measure smaller Verdet constants. For example the Verdet constant of air, in order to correct for the gap between the edges of the coil and an arbitrary sample.



(a) Oscilloscope Output



(b) Signal Amplitude VS angle

Figure 18: Simulation of Faraday signal as a function of time and polarization angle by assuming the corrected version of Malus' Law for phase. (a) Shows the oscilloscope output for the polarizer set at $\theta = 45^\circ$. Gain was kept at one, to illustrate how the lock in can isolate only 1 frequency from the noise, seen by the blue curve superposed on the black. (b) Shows the lock in output, i.e. the signal amplitude as a function of polarizer angle θ . We note the characteristic waveform pattern for the signal vs angle plot. The code to generate this plot using our `wfsim` module is found [here](#).

2. Use different types of polarizers and examine the phase shift in a similar manner as shown in Section 6.4.
3. Permanently attach the developed hardware on the Teach-spin apparatus in order to avoid vibrations and increase data acquisition speed.

All the files realted to our experiment, including lab notebook entries, raw data, annotated code, 3D models and renders can be found here: <https://github.com/PanosEconomou/advanced-lab/tree/main/2.Faraday-Rotation>.

References

- [1] F. Loeffler, "A faraday rotation experiment for the undergraduate physics laboratory," *American Journal of Physics*, vol. 51, no. 7, pp. 661–663, 1983.
- [2] L. Aplet and J. W. Carson, "A faraday effect optical isolator," *Applied Optics*, vol. 3, no. 4, pp. 544–545, 1964.
- [3] M. Weber, "Faraday rotator materials for laser systems," in *Laser and Nonlinear Optical Materials*, vol. 681, pp. 75–90, International Society for Optics and Photonics, 1987.
- [4] D. Oberoi and C. Lonsdale, "Media responsible for faraday rotation: A review," *Radio Science*, vol. 47, no. 06, pp. 1–11, 2012.
- [5] D. Staelin and E. Reifenstein III, "Faraday rotation in pulsars," *The Astrophysical Journal*, vol. 156, p. L121, 1969.
- [6] Z. Instruments, "Principles of lock-in detection and the state of the art." https://www.zinst.com/sites/default/files/li_primer_zi_whitepaper_principles_of_lock_in_detection.pdf, 2016. (Accessed on 04/13/2021).
- [7] N. F. Borrelli, "Faraday rotation in glasses," *The Journal of Chemical Physics*, vol. 41, no. 11, pp. 3289–3293, 1964.

- [8] P. R. Berman, “Optical faraday rotation,” *American Journal of Physics*, vol. 78, no. 3, pp. 270–276, 2010.
- [9] K. T. McDonald, “Faraday rotation,” *Joseph Henry Laboratories, Princeton University, Princeton, NJ 08544*, 2008.
- [10] R. Fitzpatrick, “Faraday rotation.” <http://farside.ph.utexas.edu/teaching/em/lectures/node101.html>, Feb. 2002. (Accessed on 04/06/2021).
- [11] N. Miura, “2.08 - magneto-spectroscopy of semiconductors,” in *Comprehensive Semiconductor Science and Technology* (P. Bhattacharya, R. Fornari, and H. Kamimura, eds.), pp. 256–342, Amsterdam: Elsevier, 2011.
- [12] J. H. Scofield, “Frequency-domain description of a lock-in amplifier,” *American Journal of Physics*, vol. 62, no. 2, pp. 129–133, 1994.
- [13] S. R. Kurtz, “Mixers as phase detectors,” 2001.
- [14] Z. Instruments, “Principles of lock-in detection — zurich instruments.” <https://www.zhinst.com/others/en/resources/principles-of-lock-in-detection>, Nov. 2016. (Accessed on 04/06/2021).
- [15] Teachspin, “Faraday rotation — teachspin.” <https://www.teachspin.com/faraday-rotation>, May 2015. (Accessed on 04/13/2021).
- [16] K. W. Busch and M. A. Busch, “Chapter 3 - light polarization and signal processing in chiroptical instrumentation,” in *Chiral Analysis (Second Edition)* (P. L. Polavarapu, ed.), pp. 73–151, Elsevier, second edition ed., 2018.
- [17] G. Galzerano and P. Laporta, “Modulators, optical,” in *Reference Module in Materials Science and Materials Engineering*, Elsevier, 2016.
- [18] A. B. Villaverde and D. A. Donatti, “Verdet constant of liquids; measurements with a pulsed magnetic field,” *The Journal of Chemical Physics*, vol. 71, no. 10, pp. 4021–4024, 1979.
- [19] Y. Abdelghaffar and A. Alhosani, “Verdet constant calculation for advanced lab,” 2021.

Appendix A. Faraday CLI Commands

Here we provide a complete list of the commands that clilib contains as well as their input and output description. The code for clilib can be found here: https://github.com/PanosEconomou/advanced-lab/blob/main/2.Faraday-Rotation/2.Code/Faraday_Controller/clilib.py.

Figure A.19: Command Line Application Interface for controlling the Faraday Rotation apparatus

1. set_angle

Sets the angle of the arduino by sending the appropriate integer code to it.

angle: [Required] The integer value of the angle
arduino: [Required] the serial port the arduino is in
sleep (0.001): How long to sleep after sending the message in s
VERBOSE (False): If true prints a confirmation message

2. set_speed

Sets the speed of the stepper motor by sending the appropriate integer code to it.

speed: [Required] The integer value of the speed in rpm
arduino: [Required] the serial port the arduino is in
sleep (0.001): How long to sleep after sending the message in s
VERBOSE (False): If true prints a confirmation message

3. move_to_angle

Moves the polarizer to the angle by sending the appropriate integer code to it.

angle: [Required] The integer value of the angle
arduino: [Required] the serial port the arduino is in
sleep (0.001): How long to sleep after sending the message in s
VERBOSE (False): If true prints a confirmation message

4. move_by_angle

Moves the polarizer by an angle clockwise.

angle: [Required] The integer value of the angle
arduino: [Required] the serial port the arduino is in
sleep (0.001): How long to sleep after sending the message in s
VERBOSE (False): If true prints a confirmation message

5. move_by_angle_ccw

Moves the polarizer by an angle counter clockwise.

angle: [Required] The integer value of the angle
arduino: [Required] the serial port the arduino is in
sleep (0.001): How long to sleep after sending the message in s
VERBOSE (False): If true prints a confirmation message

6. read_angle

Reads the current angle from the arduino.

arduino: [Required] the serial port the arduino is in
sleep (0.001): How long to sleep after sending the message in s
VERBOSE (False): If true prints a confirmation message

Returns:

angle: An integer of the angle obtained from the arduino

7. set_verbose

Sets the default VERBOSE value for a command to be executed

verbose (False): [Required] the VERBOSITY

8. set_sleep

Sets the default sleep value for a command to be executed

SLEEP (0.001): [Required] the sleep time in s

9. get_data_csv

Export Oscilloscope data to CSV

inst: [REQUIRED] the instrument object
channels ([1,2,3,4]): List of channels to plot
points (1000): Number of points to get data from
filename (None): The filename of the CSV (if None it defaults to timestamp)
directory (./): The directory to save the file
VERBOSE (False): When True prints the preamble

10. plot_oscilloscope

Plots the Oscilloscope Screen

inst: [REQUIRED] the instrument object
channels ([1,2,3,4]): List of channels to plot
points (1000): Number of points to get data from
dpi (200): The dpi of the image
VERBOSE (False): When True prints the preamble

11. read_monitor

Reads the contents of the serial monitor of the arduino up until the next line

12. help

Displays a list of Commands.

Appendix B. AC data collection script

Using the developed libraries *oscillovisa* and *clilib* we were able to write a script for the experimental procedure to obtain the Verdet constant of any material under test. The code for this procedure is shown below.

```
1  from oscillovisa import *
2  from clilib import *
3  from csvlib import *
4  import numpy as np
5  import matplotlib.pyplot as plt
6  from matplotlib.animation import FuncAnimation
7  import time
8  from tqdm import tqdm
9
10 # Set the run Variables
11 VERBOSE = False
12 WAIT_TIME = 0.01
13 MOTOR_SPEED = 20
14 directory = './DC_VERDET_ROD/'
15 min_angle = 0
16 max_angle = 360
17 Nangles = 360
18
19 # GET Arduino and Oscilloscope
20 arduino = get_arduino(VERBOSE=VERBOSE)
21 oscilloscope = get_intstrument(VERBOSE=VERBOSE)
22
23 angle = np.linspace(min_angle,max_angle,Nangles,dtype=int)
24 V = []
25 V_std = []
26 a_data = []
27
28 # Set the speed
29 set_angle(0,arduino,VERBOSE=VERBOSE)
30 set_speed(MOTOR_SPEED,arduino,VERBOSE=VERBOSE)
31
32 # Relevant Realtime Plotting Variables
33 fig = plt.figure(figsize = (10,7),dpi=70)
34 ax = fig.add_subplot()
35
36 ln, = plt.plot([], [], '+',c='darkblue',label='Raw Data')
37
38 # Initialises the plot
39 def init():
40     ax.set_xlabel(r'Angle $\Delta \phi$ [degrees]')
41     ax.set_ylabel(r'Voltage V [V]')
42     ax.set_title('Voltage VS Angle')
43     ax.legend(frameon=False)
44     return ln,
45
46 # The actual Experimental Procedure
47 # For all angles
48 def get_measurement(a):
49     global V,V_std
50     # Set the polariser
51     move_to_angle(a,arduino,VERBOSE=VERBOSE)
52
53     # Wait
54     time.sleep(WAIT_TIME)
55
56     # Get the measuremets
57     amplitude = get_data(oscilloscope,channel=2)
58     V.append(np.mean(amplitude[0]))
59     V_std.append(np.std(amplitude[0]))
60
61     # Save the data to CSV
62     get_data_csv(oscilloscope,channels=[1,2],directory=directory,filename='Angle-' + str(a) + '.csv')
63
64
65 # Output the values to CSV
```

```

67 def on_close(event):
68     global V,V_std
69     print('Done with experiment, exporting CSV')
70     V = np.array(V)
71     V_std = np.array(V_std)
72     create_csv(name='Voltage-Amplitude.csv',directory=directory,titles=['Angle','Voltage','Voltage_std'],
73                 ] ,data=[angle,V,V_std],VERBOSE=True)
74
75 # Perform the Run
76 for a in tqdm(angle):
77     get_measurement(a)
78
79 init()
80 dV = max(V)-min(V)
81 da = max(angle)-min(angle)
82 if dV!=0 and da!=0:
83     ax.set_xlim(min(angle)-0.1*da, max(angle)+0.1*da)
84     ax.set_ylim(min(V)-0.1*dV, max(V)+0.1*dV)
85
86 ln.set_data(angle, V)
87
88 on_close(None)
89
90 plt.savefig(directory+'Voltage-VS-Angle',dpi = 300)
91 plt.show()

```

Listing 1: Data Collection Script

Appendix C. Lock in constants for different experiments

Here we provide a detailed view of the equipment setup for the AC experiments performed. Specifically, we include constants such as the length of the samples, the coupling between the different modules of the Teachspin lock in amplifier, relevant gains, etc.

Quantity	Value (no LPF)	Value (LPF)	Quantity	Value (no LPF)	Value (LPF)
Sample					
Length	$10.174 \pm 0.005 \text{ cm}$		Length	$21.2 \pm 0.05 \text{ cm}$	
Solenoid Constant	0.011 T/A		Solenoid Constant	0.011 T/A	
Lock In constant	0.1		Lock In constant	0.1	
Sensor Resistance	$1 \text{ k}\Omega$		Sensor Resistance	$1 \text{ k}\Omega$	
Sensor Responsivity	0.6 A/W		Sensor Responsivity	0.6 A/W	
Preamplifier					
Coupling	AC	AC	Coupling	AC	AC
2nd Input	Grounded	Grounded	2nd Input	Grounded	Grounded
Gain	10	10	Gain	10	10
Low Pass filter					
Order Q	N/A	2	Order Q	N/A	2
Frequency	N/A	100 Hz	Frequency	N/A	80 Hz
Lock-in Detector					
Coupling	AC	AC	Coupling	AC	AC
Reference	Phase Shifter	Phase Shifter	Reference	Phase Shifter	Phase Shifter
Signal	Preamplifier	Low pass filter	Signal	Preamplifier	Low pass filter
Gain	20	20	Gain	20	20
Oscillator					
Amplitude	3.00 V	3.00 V	Amplitude	3.00 V	3.00 V
Frequency	36.4 Hz	36.4 Hz	Frequency	36.4 Hz	36.4 Hz
Wave	Sine	Sine	Wave	Sine	Sine
Attenuation	N/A	N/A	Attenuation	N/A	N/A
RMS Current	$480.0 \pm 0.7 \text{ mA}$	$476.8 \pm 0.8 \text{ mA}$	RMS Current	$683.1 \pm 0.2 \text{ mA}$	$476.8 \pm 0.8 \text{ mA}$
Phase Shifter					
Phase	255°	45°	Phase	256°	45°
Low Pass filter Amplifier					
Time Constant	0.03 s	0.03 s	Time Constant	0.03 s	0.03 s
Gain	20	50	Gain	50	50
Attenuation	12 dB/oct	12 dB/oct	Attenuation	12 dB/oct	12 dB/oct
Offset	-0.20 V	-0.15 V	Offset	-0.27 V	-0.37 V

Table C.4: Relevant constants related to the experimental setup for lock in detection of Verdet constant for SF-57 glass rod sample.

Table C.5: Relevant constants related to the experimental setup for lock in detection of Verdet constant for water sample.